Dynamical Model of Drug Accumulation in Bacteria: Sensitivity Analysis and Experimentally Testable Predictions

Neda Vesselinova[1, 2], Boian S. Alexandrov[1], and Michael E. Wall*[3]

[1]Theoretical Division, Los Alamos National Laboratory, Los Alamos NM 87545

[2]University of California, Los Angeles, CA 90095

[3]Computer, Computational, and Statistical Sciences Division, Los Alamos National Laboratory, Los Alamos NM 87545

*Corresponding author

November 4, 2015

LA-UR-15-28626

Abstract. We present a dynamical model of drug accumulation in bacteria. The model captures key features in experimental time courses on ofloxacin accumulation: initial uptake; short-term response; and long-term adaptation. In combination with experimental data, the model provides estimates of import and export rates in each phase, the latency in the short-term response, and the rate of increase in efflux during adaptation. Global sensitivity analysis, local sensitivity analysis, and Bayesian sensitivity analysis of the model provide information about the robustness of these estimates, and about the relative importance of different features of the accumulation time courses in three different bacterial species: *Escherichia coli*, *Staphylococcus aureus*, and *Pseudomonas aeruginosa*. The results lead to experimentally testable predictions of membrane permeability and drug efflux and trapping, which influence drug resistance. A key prediction is that an increase in *E. coli* ofloxacin accumulation is accompanied by a decrease in membrane permeability, suggesting that, depending on changes in other factors, decreasing permeability is not always an effective drug resistance strategy.

Author Summary. Bacteria live or die depending on how much antibiotic gets inside them. Using a simple mathematical model, detailed information about drug import and export can be teased out of time courses of internal drug levels after a sudden environmental exposure. The results reveal that blocking diffusion across the membrane is not always an effective drug resistance strategy for bacteria.

Introduction

Drug resistance in bacteria can be increased by efflux pump systems [1], and pump inhibition has emerged as a strategy for overcoming drug resistance [2]. Many details of how efflux pumps work are still unclear, however. In particular, quantitative information about how efflux influences drug accumulation in bacteria is still scarce [3].

Drug accumulation is a key factor in obtaining a quantitative understanding of resistance. For example, predictions of minimum inhibitory concentrations (MICs) of β-lactams in *Escherichia coli* were obtained by equating the steady state periplasmic drug concentration with a periplasmic binding protein inhibitory concentration [4]. A predicted MIC was calculated as the *external* concentration that would yield the accumulated *internal* inhibitory concentration in steady state, considering flux terms from membrane permeation and β-lactamase degradation. MIC predictions also have been made considering the action of efflux pumps on cephalosporins [5] and β-lactams [6] in *E. coli*. These predictions were accompanied by estimates of efflux pump Michaelis-Menten kinetic constants (*i.e.*, K_m and k_{cat} values), providing an explicit connection between efflux and resistance.

Time-dependent drug accumulation studies also have yielded insight into drug transport [7-9]. Diver et al. [8] found exposure of *E. coli* to five different quinolones induced a rapid ~10 sec uptake followed by a ~30 min phase of more gradual

accumulation. Similar two phase behavior was seen by Asuquo and Piddock [7] in accumulation of fifteen different quinolones in *E. coli*, *Pseudomonas aeruginosa*, and *Staphylococcus aureus* [7]. Whereas drug levels appeared to plateau in *E. coli* and *S. aureus*, levels in *P. aeruginosa* gradually decreased at longer times, suggesting an adaptation process [7].

Mathematical modeling has provided substantial insights into accumulation of beta-lactams [4,6], cephalosporins [5], and tetracycline [9] in *E. coli*. Quinolone accumulation, however, has not yet been analyzed in the context of a mathematical model. Here we present a mathematical model of drug accumulation and use it to analyze experimental data on accumulation of the quinolone oxfloxacin in *E. coli*, *S. aureus*, and *P. aeruginosa* [7]. The analysis yields estimates of permeation and efflux rates, the latency in the short-term response, and the rate of increase in efflux during adaptation. We also perform global sensitivity analysis, local sensitivity analysis, and Bayesian sensitivity analysis of the model. The sensitivity analyses provide information about the robustness of parameter estimates and enable assessment of the relative importance of the short-term response and long-term adaptation in different bacterial species.

The results lead to experimentally testable predictions of membrane permeability and drug efflux and trapping, which influence drug resistance. A key prediction is that an increase in *E. coli* drug accumulation is accompanied by a decrease in membrane permeability, illustrating that decreasing permeability, although

commonly associated with increased drug resistance [10], is not always an effective drug resistance strategy for bacteria. Overall the results indicate the utility of mathematical modeling and sensitivity analysis in obtaining new insights into drug accumulation in bacteria.

Results

Model behavior

Our model of drug accumulation (Methods) was designed to describe two phases of drug accumulation dynamics, with long-term adaptation in the second phase (Fig. 1). After exposure at $t = 0$, the first phase begins, where cellular antibiotic levels rise and relax toward an asymptotic value a_1. The relaxation in this phase is exponential with rate β_1. At time $t = \tau$, the second phase begins, where antibiotic levels may either rise or fall towards a new asymptotic value a_2. The relaxation in this phase is initially dominated by exponential relaxation with rate β_2. Later, adaptation can dominate the dynamics, following $[1+ \delta(t- \tau)]^{-1}$. Together these features capture the full set of behaviors exhibited by the experimental data on ofloxacin accumulation [7] (Fig. 2).

Parameter estimates

107 Parameter values were estimated by fitting the model to data on ofloxacin
108 accumulation in *E. coli*, *P. aeruginosa*, and *S. aureus*. Following Ref. [7], the fits were
109 performed assuming a uniform measurement error. (Rough error estimates for the
110 data, inferred from the values given for the norfloxacin, are: 4.6 ng/mg for *E. coli*; 1.5
111 ng/mg for *P. aeruginosa*; and 8.7 ng/mg for *S. aureus*.) Reasonable fits were
112 obtained for all datasets (Fig. 2). Parameter values varied substantially for different
113 bacteria (Table 1), as expected given the differing behaviors. *E. coli* exhibits two
114 phases of accumulation with little apparent long-term adaptation, consistent with
115 the low value of δ. *P. aeruginosa* shows a stronger adaptation response,
116 corresponding to the higher value of δ. *S. aureus* exhibits a single phase response
117 without adaptation, consistent with the value of τ being greater than the longest
118 time point.
119
120 ***Sensitivity analysis results***
121
122 Sensitivity analysis is a technique for evaluating how variations in the output of a
123 mathematical model are related to variations in the model inputs. We used
124 sensitivity analysis to assess the importance of different model parameters in
125 determining the antibiotic accumulation behavior. We performed three independent
126 analyses using: global sensitivity analysis (GSA), local sensitivity analysis (LSA), and
127 Bayesian sensitivity analysis (BSA). For each analysis, the time courses using the
128 optimal parameter values were used as reference behaviors.
129

130 *Global sensitivity analysis*. GSA explores the sensitivity of the model output within
131 the entire (prior) parameter space of the model inputs. We performed variance-
132 based GSA [11], which decomposes the variance of the output into parts ascribed to
133 different input parameters using a Fourier Haar decomposition [12,13]. Both the
134 "total effect" and "main effect" for each input parameter were calculated using the
135 Sobol Monte Carlo algorithm [14]; here we focus on the total effect results. The prior
136 range of the input parameters was defined using uniform logarithmic distributions
137 given in Table 2.
138
139 GSA results for *E. coli*, *P. aeruginosa*, and *S. aureus* are shown in Figure 3. For *E. coli*,
140 β_1 exerts the highest total effect initially, followed by a_1, τ, and a_2. The effect of β_2
141 never dominates, but is substantial at early times. The sensitivity to δ is low at all
142 times. For *P. aeruginosa*, a_1 exerts the highest total effect initially, followed by τ and
143 a_2. In contrast with *E. coli*, the sensitivity to δ is high for *P. aeruginosa*, while both β_1
144 and β_2 show low sensitivity. For *S. aureus*, β_1 exerts the highest total effect early on,
145 shifting to a_1 and then τ at later times. The effects of a_2 and β_2 are smaller by
146 comparison. Like for *E. coli*, the sensitivity to δ is low.
147
148 *Local sensitivity analysis*. LSA has a rich history of use in assessing the robustness of
149 biochemical network model behavior to changes in parameter values [15,16]. In LSA,
150 the local gradients of the model output are calculated with respect to model
151 parameters at a fixed point. Here we use the gradients to define a covariance matrix
152 of variations [17] (Methods), and interpret the LSA in terms of the eigenvalues and

153 eigenvectors of the covariance matrix. Small eigenvalues are associated with
154 parameter combinations that show higher sensitivity.
155
156 We performed LSA on the *P. aeruginosa* model, for comparison to the GSA. Each
157 eigenvector in the LSA is strongly associated with a single parameter (Fig. 4a),
158 facilitating the interpretation. The three smallest eigenvalues (Fig. 4b) are those
159 associated with a_1, a_2, and δ (corresponding to eigenvectors 1-3 in Fig. 4a),
160 indicating that the sensitivity of the model to these parameters is relatively high.
161 The parameters β_1, β_2 and τ are associated with orders of magnitude higher
162 eigenvalues, indicating that the sensitivity to these parameters is relatively low.
163
164 *Bayesian sensitivity analysis*. BSA estimates the probability density functions
165 (pdf's) of the model parameters given observed data and measurement errors using
166 Bayes' theorem [18,19]. Like GSA, BSA requires prior distributions of the model
167 inputs. The more sensitive is the model parameter, the more constrained is the
168 posterior pdf compared to the prior pdf.
169
170 Figure 5 shows Bayesian sensitivity analysis for the *P. aeruginosa* model. Here, the
171 Bayesian analysis identifies a Markov-Chain Monte Carlo (MCMC) sample of models
172 that are consistent with the observed data, assuming a uniform measurement error [7].
173 The histograms along the diagonal represent the posterior pdf's of the model parameters
174 constrained by the model observations. Each dot in the off-diagonal scatter plots
175 represents a model-parameter set from the final MCMC sample. Some of the parameters,

a_1, a_2, and δ appear to have peaked distributions, indicating a sharpened sensitivity within the posterior range. The probability density of τ is uniform at longer times and zero at shorter times. The distributions of β_1 and β_2 are flat, and, therefore they are less sensitive parameters. The scatter plot between a_2 and δ is extended along the a_2-δ direction, indicating that these parameters are correlated.

Experimentally testable predictions of permeability and efflux

We used Eqs. (5) and (6) to predict permeability and efflux given the estimated parameters. The predictions are quantified in the form of the efflux rate, $\varepsilon(t)$, which is defined as the portion of the specific export rate not associated with permeation, and the accumulation factor, $\phi(t)$, which is defined as $\alpha(t)/\beta(t)$, the ratio of the permeability to the export rate. Depending on the sign of $\varepsilon(t)$, qualitatively different mechanisms are at work: a positive value is associated with efflux, while a negative value is associated with trapping.

The resulting predictions of $\varepsilon(t)$ and $\phi(t)$ are shown in Table 4. The robustness of these predictions depends on the robustness of the estimation of a_1 and β_1, for $t<\tau$, and a_2 and β_2, for $t=\tau$. According to the sensitivity analysis, the estimates of some of these parameters are not robust, yielding unreliable predictions for some of the *P. aeruginosa* and *S. aureus* values. For completeness, the unreliable predictions are listed in Table 4, but are enclosed in parentheses.

Discussion

198

199 ***Interpretation of sensitivity analysis results***

200

201 *Global Sensitivity Analysis:* Results obtained using the GSA suggest that the relative
202 importance of the various model parameters in determining the output behavior of
203 the simulations differs for *E. coli*, *P. aeruginosa*, and *S. aureus* (Figure 3). However,
204 there are also some similarities. In most cases, a_1 and β_1 are important only at very
205 early-times right at the beginning of the data collection. This suggests that proper
206 estimation of a_1 and β_1 requires accurate early-time measurements. In all cases, the
207 sensitivity of a_1 and β_1 diminishes over time. Also in all cases, the sensitivity of a_1
208 increases with time. The temporal behavior of β_2 sensitivity is very different in all
209 three cases: β_2 is relatively important at early times for the case of *E. coli*; β_2 is
210 unimportant for the case of *P. aeruginosa*; and the β_2 sensitivity peaks at the mid-
211 times for the case of *S. aureus*. Interestingly, the parameter δ is important only for
212 the case of *P. aeruginosa*. The temporal behavior of τ sensitivity is similar for the
213 case of *E. coli* and *P. aeruginosa* (τ sensitivity is decreasing with time), but very
214 different for the case of *S. aureus* (τ sensitivity is increasing with time).

215

216 *Local sensitivity analysis:* The global and local sensitivity analyses yield similar
217 results for *P. aeruginosa*. Both analyses identify a_1, a_2, and δ as sensitive model
218 parameters. However, the global and local sensitivity analyses produce different
219 sensitivity estimates related to the parameter τ. The model is sensitive to this

220 parameter according to GSA but not according to LSA. This suggests that when all
221 the model parameters are at their optimal values, small deviations in τ values have a
222 small impact on the optimal solution. However, away from the optimal point in the
223 parameter space, τ is an important parameter in determining the model behavior.
224
225 *Bayesian sensitivity analysis:* BSA provides information how well the model
226 parameters are constrained. For the case of *P. aeruginosa* (Fig 5), the parameters a_1,
227 a_2, δ and τ are well-constrained and, therefore, sensitive model parameters. This is
228 consistent with GSA, which is expected because both analyses are global in their
229 nature. BSA also suggests correlation between estimates for a_2 and δ. The other
230 model parameters are not correlated. The correlation is supported by the similarity
231 in the time dependence of a_2 and δ sensitivities as shown in Figure 3b. Some of the
232 parameters, a_1, a_2, and δ, have peaked posterior distributions, indicating a most
233 probable value at the maximum. The parameter τ is considered to be sensitive
234 because the posterior range (from ~1.6 to ~1.68) is smaller than the prior range (0
235 – 4; all the values are $\log_{10}$ transformed and presented in Tables 2 and 3). However,
236 the posterior distribution within this range is relatively flat (i.e. uniform). The flat
237 distribution leads to a small sensitivity of the model to changes in this parameter
238 using LSA.
239
240 ***Interpretation of predictions of permeability and efflux***
241

242 For *E. coli*, the values of the accumulation factor $\phi>1$ indicate trapping of antibiotic.
243 The trapping is weak for $t<\tau$ and becomes stronger at $t=\tau$. The greater magnitude of
244 α compared to ε values indicates that the permeability dominates the response. For
245 *P. aeruginosa*, the values of $\phi<1$ indicate that efflux of antibiotic is important. For *S.*
246 *aureus*, the value $\phi>1$ indicates a net trapping of antibiotic, like *E. coli*. In contrast to
247 *E. coli*, the comparable magnitudes of α and ε indicate that permeability and
248 trapping are roughly equally important in during the whole time course.
249
250 The predictions suggest efflux is unimportant in the response of *E. coli* and *S. aureus*
251 to ofloxacin. Permeation and trapping instead dominate the response. In contrast,
252 efflux is predicted to be important in the response of *P. aeruginosa* to ofloxacin. The
253 initial accumulation is less than what would be expected by permeation alone,
254 indicating an efflux effect. In addition, the antibiotic level slowly decreases after the
255 initial uptake, indicating an increase of efflux with time, presumably due to an
256 adaptive response involving pump production.
257
258 The predictions for *E. coli* are especially intriguing. The response involves a ~50-
259 fold decrease in permeability about 800 seconds after exposure, which would
260 naively be expected to increase resistance [10]. However, the decrease in
261 permeability is accompanied by a ~10-fold decrease in trapping. Because the
262 decrease in trapping is less than the decrease in permeability, the result is an
263 increase, rather than a decrease, in antibiotic accumulation.
264

265 Similar to the subtle connection found here between permeability and resistance,
266 Nagano and Nikaido [5] used mathematical modeling to show how efflux pump
267 deletion or overexpression might not change the MIC value of strong efflux pump
268 substrates. It is interesting to consider these findings in light of a recent survey of
269 physical properties of active compounds in a drug screening collection and their
270 relation to whole cell antibacterial activity [20]. The survey reported on the
271 difficulties encountered in simultaneously optimizing both biochemical potency and
272 antibacterial activity, and concluded that "what is clearly needed is greater insight
273 into medicinal chemistry strategies which optimize transport through porins and
274 decrease efflux through the prolific efflux pumps." Together, the findings reported
275 here and elsewhere [5,6] suggest that mathematical modeling of permeation and
276 efflux can be a key tool in enabling antibacterial medicinal chemistry.
277
278 Our results indicate that detailed, quantitative analysis of antibiotic accumulation
279 time courses using mathematical modeling can yield new insights and
280 experimentally testable predictions about mechanisms of drug resistance. The
281 sensitivity analysis provides basis for distinguishing important from unimportant
282 predictions. The predictions imply that decreasing permeability is not always an
283 effective strategy for bacteria to increase drug resistance. This outcome in particular
284 provides an example of the potential pitfalls involved in reasoning about structure-
285 function relations in biochemical networks [21], and reinforces the need for
286 incorporating mathematical modeling into strategies for fighting drug resistance.

Overall this study illustrates the key role that mathematical modeling and sensitivity analysis can play in deep interpretation of experimental data in biology.

Materials and Methods

Model

The time dependence of accumulated drug *a(t)* is modeled using

$$\frac{da(t)}{dt} = \alpha(t)a_o - \beta(t)a(t) \tag{1}$$

where a_o is the environmental antibiotic concentration, α(t) is the specific import rate, and β(t) is the specific export rate. Here and elsewhere the terms "import" and "export" refer to combined effects of passive and active transport, and the term "specific" is sometimes used to indicate that the rate constant is multiplied by the antibiotic concentration. Both α(t) and β(t) may change depending on the phase of the response. The import rate α(t) is given by

$$\alpha(t) = \begin{cases} \alpha_1, & t < \tau \\ \alpha_2, & t \geq \tau \end{cases}, \tag{2}$$

where α_1 applies to the initial phase of the accumulation dynamics ($t<\tau$), and α_2 applies to the later phase ($t \geq \tau$).

The export rate β(t) is given by

$$\beta(t) = \begin{cases} \beta_1, & t < \tau \\ \beta_2[1 + \delta(t - \tau)], & t \geq \tau \end{cases}, \tag{3}$$

where β_1 applies during the initial phase ($t<\tau$), β_2 applies during the later phase ($t\geq\tau$), and δ is the fractional rate of increase of export during the later phase.

Assuming $\delta << \beta_2$ and $\delta(t - \tau) \ll 1$ yields

$$a(t) = \begin{cases} e^{-\beta_1 t}a(0) + \left(1 - e^{-\beta_1 t}\right)a_1, & t \leq \tau \\ e^{-\beta_2(t-\tau)}a(\tau) + \left[1 - e^{-\beta_2(t-\tau)}\right]\dfrac{a_2}{1 + \delta(t - \tau)}, & t > \tau \end{cases} \tag{4}$$

where $a_1 = \alpha_1 a_o / \beta_1$, and $a_2 = \alpha_2 a_o / \beta_2$.

Given additional assumptions, the α and β parameters can be used to derive permeation and efflux or trapping rates (see below). The δ parameter models long-term adaptation by, e.g., gene regulation.

Parameter estimation

325 Parameter estimation for Eq. (4) was performed using published experimental time
326 courses of ofloxacin accumulation in *E. coli*, *P. aeruginosa*, and *S. aureus* [7]. Data
327 points were extracted from Figure 1 in Ref. [7]. Numerical solutions to Eq. (4) were
328 obtained for each data point using functions defined in Mathematica Version 10
329 (Wolfram Research, Inc., Champaign, IL). As the estimated errors were the same for
330 all data points [7], an unweighted mean squared deviation (MSD) between the
331 model and the data was used as a target function for fitting. The MSD was minimized
332 with respect to values of a_1, a_2, β_1, β_2, δ, and τ using the `FindMinimum` method,
333 assuming a(0)=0. The values of a_1, a_2, β_1, β_2, δ were varied over twelve decades. For
334 *E. coli* and *P. aeruginosa*, the value of τ was varied from 0-10,000 s (covering the full
335 span of each 3,600 s time course) to seek an optimal solution. For *S. aureus*,
336 optimization was performed for τ = 10,000 s. Mathematica workbooks and
337 experimental data for all cases are available in a compressed archive in the
338 Supporting Information.
339
340 ***Sensitivity analysis methods***
341
342 All analyses were performed using the open source code Model-Analysis and
343 Decision Support (MADS), developed at Los Alamos National Laboratory
344 (http://mads.lanl.gov).
345
346 *Global Sensitivity Analysis (GSA)*: For our analysis, we used the Sobol Monte Carlo
347 algorithm [14]. The algorithm estimates the total and main effect for each model

parameter. The total effect is the total contribution to the output model variance to a given model parameter, including all the combined effects caused by its interactions with any other model parameter. The main effect measures the impact of varying a single model parameter by itself. The total and main effect can be very similar when the model parameters are independent. Sobol Monte Carlo algorithm was performed using about 10^6 independent model evaluations. Additional analyses (not presented) demonstrated that the number of model evaluations is sufficient to achieve converges for the estimate quantities.

Local Sensitivity Analysis (LSA): We used a finite difference method requiring a limited number of model evaluations (equal to the number of unknown parameters). As a result, we obtain a gradient matrix **J** (i.e. the Jacobian) with dimensions [$m \times n$] where m is the number of model parameters and n is the number of model inputs. Each component of the **J** matrix represents the local sensitivity of each model parameter to each model output [17]. We analyze the covariance matrix **C** of model parameters which is computed as $\mathbf{C} = [J^T J]^{-1}$. The covariance matrix is frequently analyzed using eigenanalysis where eigenvectors and eigenvalues of the covariance matrix are explored. How dominant (important) is each eigenvector depends on the respective eigenvalues; the smaller the eigenvalue, the higher the importance of the eigenvector. The components of each eigenvector represent the contributions of each model parameter to the simultaneous variation of multiple parameters: the larger the absolute value of the components, the larger the contribution. Model parameters with large contribution in dominant eigenvectors are important

371 (sensitive) model parameters. Model parameters with large contribution in non-
372 dominant eigenvectors are also unimportant (insensitive) model parameters. If
373 several model parameters have important contribution in a single eigenvector, these
374 model parameters are correlated. If these contributions have the same sign, the
375 correlation is positive. If these contributions have opposite signs, the correlation is
376 negative.
377
378 *Bayesian Sensitivity Analysis (BSA)*: The BSA was performed using the Robust
379 Adaptive Metropolis Markov Chain Monte Carlo algorithm [22]. To assess the
380 sensitivity of the model parameters to the model outputs we compared the prior
381 and the posterior pdf's of the model parameters (Table 2 and 3, respectively). High
382 sensitivity parameters show a posterior pdf that is substantially narrower than the
383 prior pdf.
384
385 ***Prediction of permeability and efflux***
386
387 Estimation of the model parameters enables prediction of permeability and efflux
388 rates. Given a_o, the specific import rates may be calculated as $\alpha_1 = a_1\ \beta_1/a_o$, and $\alpha_2 =$
389 $a_2\ \beta_2/a_o$. Assuming the import is due to permeation, α_1 and α_2 are the permeabilities.
390 Next, assume the specific export rate $\beta(t)$ is a sum of contributions from
391 permeability, $\alpha(t)$ and other effects, $\varepsilon(t)$, leading to
392

$$\varepsilon(t) = \begin{cases} \beta_1 - \alpha_1, & t < \tau \\ \beta_2[1 + \delta(t - \tau)] - \alpha_2, & t \geq \tau \end{cases}. \quad (5)$$

When ε(t)>0, outward flow is enhanced compared to permeation, and ε(t) is associated with efflux. When ε(t)<0, the outward flow is decreased compared to permeation, and ε(t) is associated with trapping. The accumulation factor ϕ(t) = α(t)/β(t) is used as a measure of the importance of efflux or trapping. It is given by

$$\phi(t) = \begin{cases} a_1/a_o\,, & t < \tau \\ a_2/a_o\,[1 + \delta(t - \tau)], & t \geq \tau \end{cases}. \quad (6)$$

Eqs. (5) and (6) are only valid under the same assumptions as for Eq. (4).

Predictions of ε(t) are only meaningful using reliable estimates of both a_1 and β_1 for $t < \tau$, or both a_2 and β_2 for $t \geq \tau$. In contrast, ϕ(t) can be predicted without estimates of β_1 or β_2.

The predictions involve information about the environmental drug concentration and the conversion of estimates a_1 and a_2 from ng/mg dry weight units (Table 1) to mg/L units. The environmental ofloxacin concentration in the experiments was 10 mg/L [7]. To convert a_1 and a_2 to mg/L units, following Ref. [23], we used a buoyant density of 1.1 g/mL and a 31% dry weight for *E. coli*, a buoyant density of 1.2 g/mL and a 48% dry weight for *P. aeruginosa* (transferred from *P. putidae*), and assume a buoyant density of 1.1 g/mL and a 40% dry weight for *S. aureus*. This yielded

413 conversion factors of 0.341 mg dry weight/L for *E. coli*, 0.528 mg dry weight/L for *P.*
414 *aeruginosa*, and 0.440 mg dry weight/L for *S. aureus*.
415
416
417 **Acknowledgments**
418
419 This study was supported by the US Department of Energy under Contract DE-
420 AC52-06NA25396 through the Laboratory-Directed Research and Development
421 Program at Los Alamos National Laboratory under project number 20140121DR,
422 Combating Antibiotic Resistance: Targeting Efflux Pump Systems at Multiple Scales.
423
424 **References**
425
426 1. Li XZ, Nikaido H (2009) Efflux-mediated drug resistance in bacteria: an update.
427 Drugs 69: 1555-1623.
428 2. Kourtesi C, Ball AR, Huang YY, Jachak SM, Vera DM, et al. (2013) Microbial efflux
429 systems and inhibitors: approaches to drug discovery and the challenge of
430 clinical implementation. Open Microbiol J 7: 34-52.
431 3. Nikaido H, Pages JM (2012) Broad-specificity efflux pumps and their role in
432 multidrug resistance of Gram-negative bacteria. FEMS Microbiol Rev 36: 340-
433 363.
434 4. Nikaido H, Normark S (1987) Sensitivity of Escherichia coli to various beta-
435 lactams is determined by the interplay of outer membrane permeability and
436 degradation by periplasmic beta-lactamases: a quantitative predictive
437 treatment. Mol Microbiol 1: 29-36.
438 5. Nagano K, Nikaido H (2009) Kinetic behavior of the major multidrug efflux pump
439 AcrB of Escherichia coli. Proc Natl Acad Sci U S A 106: 5854-5858.
440 6. Lim SP, Nikaido H (2010) Kinetic parameters of efflux of penicillins by the
441 multidrug efflux transporter AcrAB-TolC of Escherichia coli. Antimicrob
442 Agents Chemother 54: 1800-1806.
443 7. Asuquo AE, Piddock LJ (1993) Accumulation and killing kinetics of fifteen
444 quinolones for Escherichia coli, Staphylococcus aureus and Pseudomonas
445 aeruginosa. J Antimicrob Chemother 31: 865-880.

8. Diver JM, Piddock LJ, Wise R (1990) The accumulation of five quinolone antibacterial agents by Escherichia coli. J Antimicrob Chemother 25: 319-333.
9. Thanassi DG, Suh GS, Nikaido H (1995) Role of outer membrane barrier in efflux-mediated tetracycline resistance of Escherichia coli. J Bacteriol 177: 998-1007.
10. Schweizer HP (2012) Mechanisms of antibiotic resistance in Burkholderia pseudomallei: implications for treatment of melioidosis. Future Microbiol 7: 1389-1399.
11. Sobol' IM (1990) On sensitivity estimation for nonlinear mathematical models. Matematicheskoe Modelirovanie 2: 112-118.
12. Sobol' IM (1993) Asymmetric convergence of approximations of the Monte Carlo method. Computational mathematics and mathematical physics 33: 1391-1396.
13. Saltelli A, Andres TH, Homma T (1993) Sensitivity Analysis of Model Output - an Investigation of New Techniques. Computational Statistics & Data Analysis 15: 211-238.
14. Saltelli A, Ratto M, Andres T, Campolongo F, Cariboni J, et al. (2008) Global Sensitivity Analysis: The Primer: John Wiley & Sons.
15. Savageau MA (1976) Biochemical systems analysis: a study of function and design in molecular biology. Reading, MA: Addison-Wesley.
16. Savageau MA (2013) System design principles. In: Wall ME, editor. Quantitative Biology: From Molecular to Cellular Systems. Boca Raton: Taylor and Francis. pp. 23-49.
17. Gustafson P, Srinivasan C, Wasserman L (1995) Local sensitivity analysis. Bayesian Statistics 5: 631-640.
18. Oakley JE, O'Hagan A (2004) Probabilistic sensitivity analysis of complex models: a Bayesian approach. J Roy Stat Soc B 66: 751-769.
19. Weiss R (1996) An approach to Bayesian sensitivity analysis. J Roy Stat Soc B 58: 739-750.
20. Brown DG, May-Dracka TL, Gagnon MM, Tommasi R (2014) Trends and exceptions of physical properties on antibacterial activity for Gram-positive and Gram-negative pathogens. J Med Chem 57: 10144-10161.
21. Wall ME (2011) Structure-function relations are subtle in genetic regulatory networks. Math Biosci 231: 61-68.
22. Vihola M (2012) Robist adaptice Metropolis algorithm with coerced acceptance rate. Stat Comp 22.
23. Bratbak G, Dundas I (1984) Bacterial dry matter content and biomass estimations. Appl Environ Microbiol 48: 755-757.

Figures

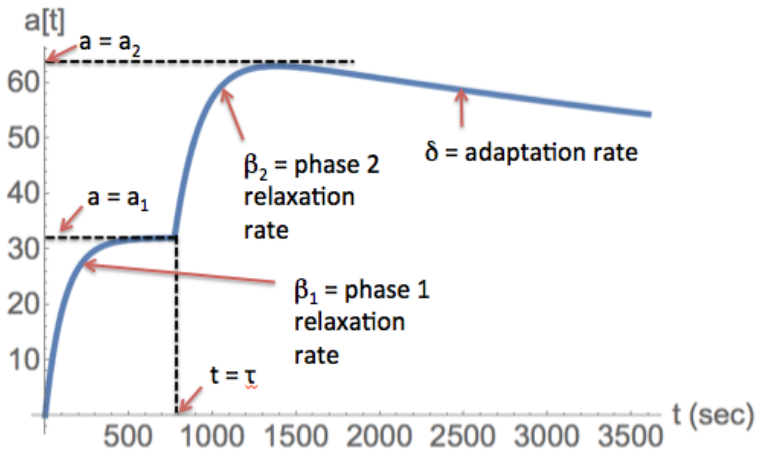

Figure 1. Behavior of the model and connection to model parameters.

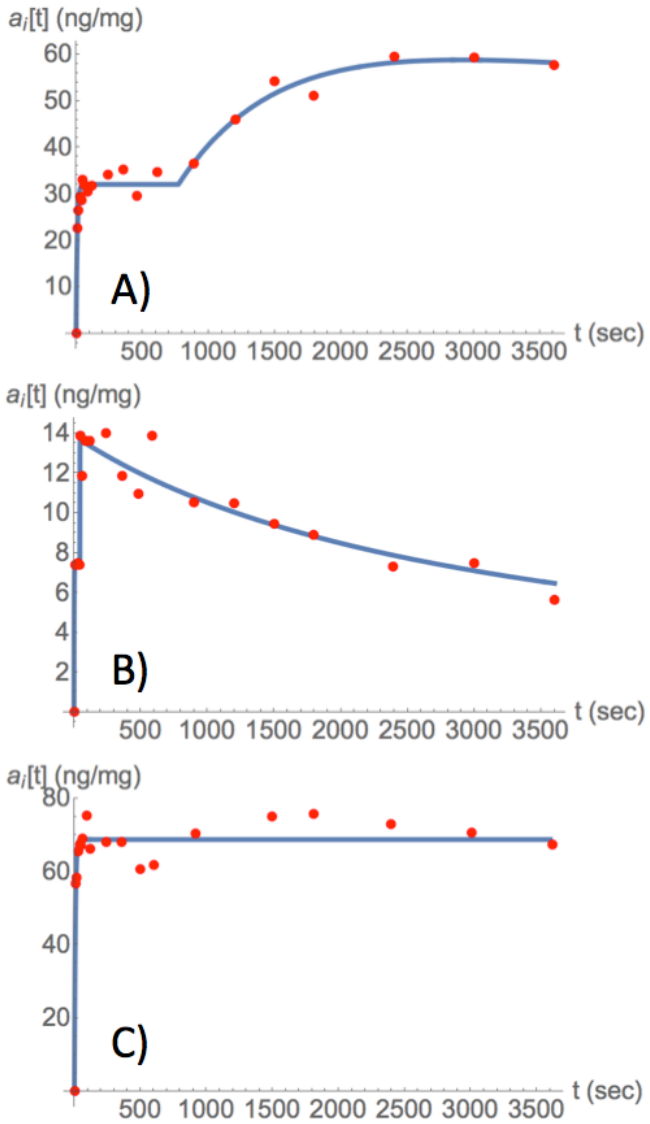

Figure 2. Fits of models to ofloxacin accumulation data. A) *E. coli*. B) *P. aeruginosa*. C) *S. aureus*. Following Ref. [7], the data are assumed to have a uniform measurement errors: 4.6 ng/mg for *E. coli*; 1.5 ng/mg for *P. aeruginosa*; and 8.7 ng/mg for *S. aureus.*

A)

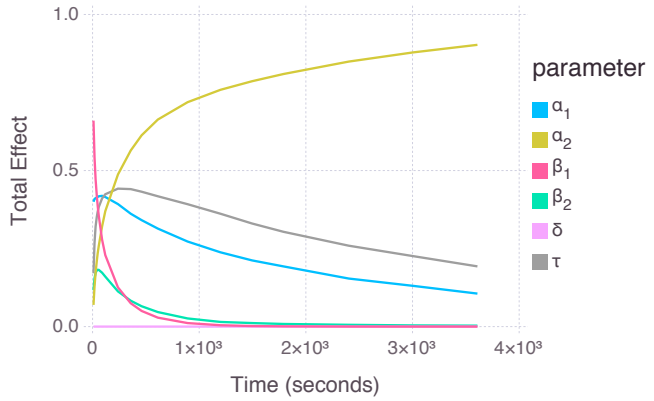
1.0
0.5
0.0
Total Effect
0
1×10³
2×10³
3×10³
4×10³
Time (seconds)
parameter
α1
α2
β1
β2
δ
τ

B)

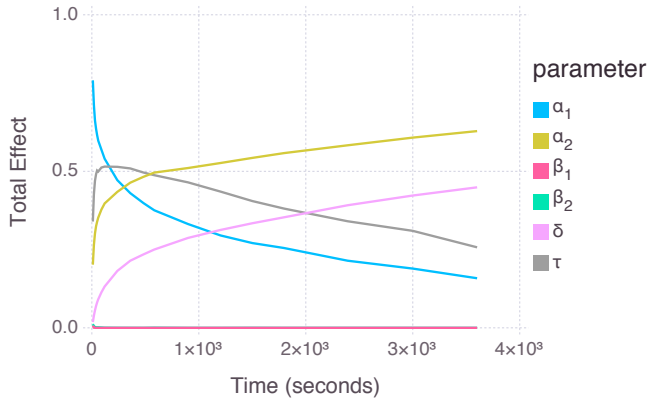
1.0
0.5
0.0
Total Effect
0
1×10³
2×10³
3×10³
4×10³
Time (seconds)
parameter
α1
α2
β1
β2
δ
τ

C)

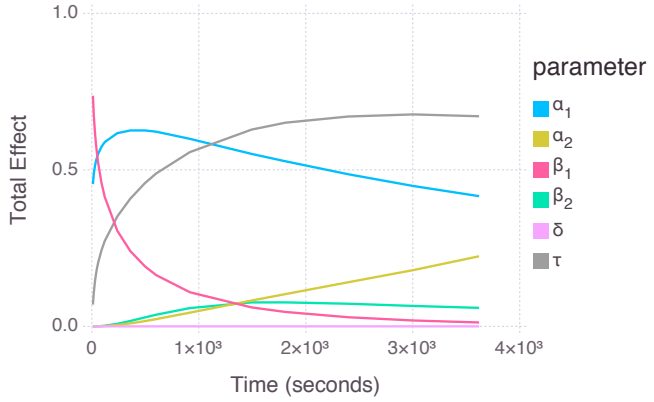
1.0
0.5
0.0
Total Effect
0
1×10³
2×10³
3×10³
4×10³
Time (seconds)
parameter
α1
α2
β1
β2
δ
τ

508 Figure 3. Global sensitivity of the model behavior to changes in parameter values for

509 A) *E. coli*, B) *P. aeruginosa*, and C) *S. aureus* models. Sensitivity is quantified using

510 the total effect measure in GSA. Color code: a_1 (cyan); a_2 (yellow); β_1 (red); β_2

511 (green); δ (pink); and τ (grey).

512

513

514

A)

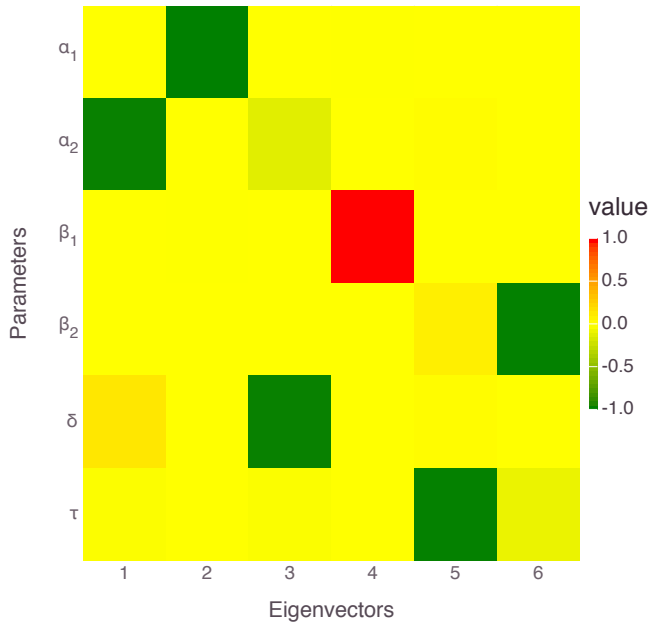

B)

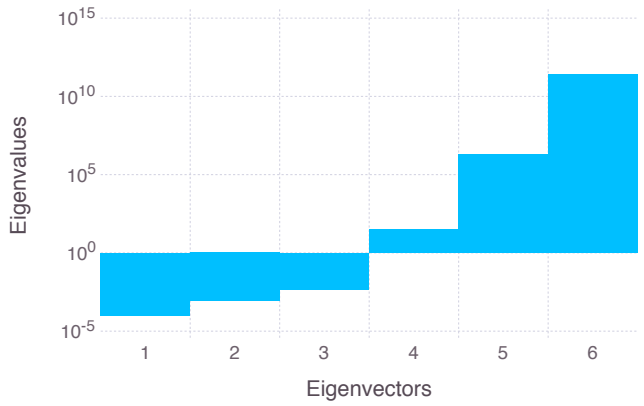

Figure 4. Local sensitivity analysis for *P. aeruginosa*. (A) Eigenvector components associated with each model parameter. (B) Eigenvalues for each eigenvector, numbered in decreasing importance from left to right. The LSA identifies a_2 as the most important model parameter because it contributes strongly to eigenvector 1,

and identifies β_2 as the least important because it contributes strongly to eigenvector 6.

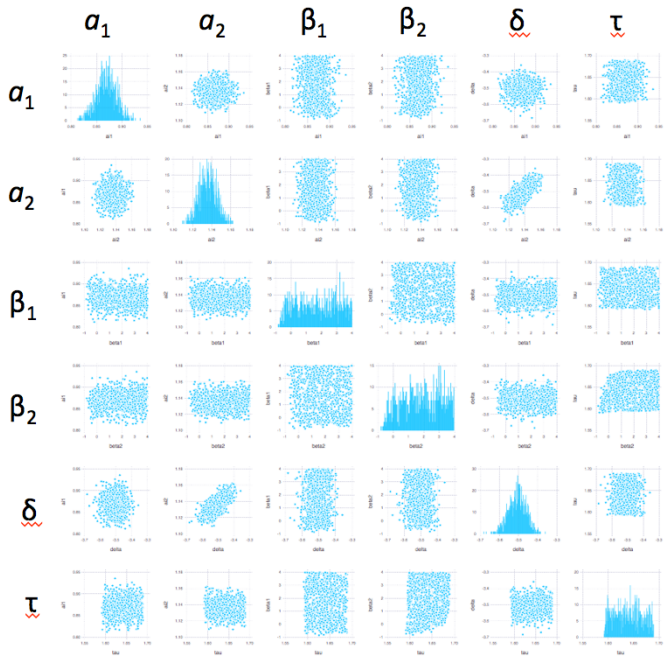

Figure 5. Bayesian sensitivity analysis for *P. aeruginosa*. The histograms along the diagonal represent the posterior pdf's of the model parameters constrained by the model observations. Off-diagonal subplots are scatter plots where each dot is a model-parameter set from the final MCMC sample. The horizontal axes define the parameter ranges (Table 3). The vertical axes along the diagonal plots define the frequency of occurrence. The vertical axes along the off-diagonal plots also define the parameter ranges (Table 3).

537 **Tables**

538

539 Table 1. Estimated parameter values obtained after fitting the model to data on

540 ofloxacin accumulation in different bacteria.

	a_1 (ng/mg)	a_2 (ng/mg)	β_1 (1/s)	β_2 (1/s)	δ (1/s)	τ (s)
E. coli	32.0	67.1	0.116	0.00125	(0.0000484)	772
P. aeruginosa	7.43	13.7	(0.682)	(3.01)	0.000314	44.5
S. aureus	68.71	(16.8)	0.149	(0.0119)	(0)	(10^4)

541

542 [a]Numbers in parentheses are unreliable according to the sensitivity analysis. They

543 are included only for completeness.

544

Table 2. Prior parameter ranges ($\log_{10}$ transformed values).

	a_1 (ng/mg)	a_2 (ng/mg)	β_1 (1/s)	β_2 (1/s)	δ (1/s)	τ (s)
min	0	0	-1	-1	-7	0
max	2	2	4	4	0	4

550 Table 3. Posterior parameter ranges based on Bayesian sensitivity analysis for *P*.

551 *aeruginosa* ($\log_{10}$ transformed values).

552

	a_1 (ng/mg)	a_2 (ng/mg)	β_1 (1/s)	β_2 (1/s)	δ (1/s)	τ (s)
min	0.8	1.11	-1	-1	-3.65	1.6
max	0.92	1.16	4	4	-3.4	1.68

553

554

555 Table 4. Predicted accumulation factors (ϕ), permeabilities (α), and efflux ($\varepsilon > 0$) or

556 trapping ($\varepsilon < 0$) rates.

557

	$\phi(t<\tau)$	$\phi(t=\tau)$	α_1 (1/s)	α_2 (1/s)	$\varepsilon(t<\tau)$ (1/s)	$\varepsilon(t=\tau)$ (1/s)
E. coli	1.09	2.29	0.13	0.0029	-0.011	-0.0016
P. aeruginosa[a]	0.39	0.72	(0.27)	(2.2)	(0.41)	(0.83)
S. aureus[a]	3.02	(0.74)	0.45	(0.01)	-0.30	(0.0031)

558

559 [a]Numbers in parentheses are unreliable according to the sensitivity analysis. They

560 are included only for completeness.

561

562

563